Available online at www.sciencedirect.com
SCIENCE DIRECT
Tetrahedron
Tetrahedron 62 (2006) 2927–2935

Regioselective hydroxylation of phenols by simultaneous photochemical generation of phenol cation-radical and hydroxyl radical

Daniel Collado,[a] Ezequiel Perez-Inestrosa,[a,*] Rafael Suau[a] and Juan T. Lopez Navarrete[b]

[a]*Department of Organic Chemistry, Faculty of Sciences, University of Málaga, 29071 Málaga, Spain*
[b]*Department of Physical Chemistry, Faculty of Sciences, University of Málaga, 29071 Málaga, Spain*

Received 10 October 2005; revised 16 December 2005; accepted 4 January 2006

Available online 19 January 2006

Abstract—Substituted phenols having pendant isoquinoline *N*-oxide were synthesized and their photochemical and luminiscent properties studied. Photolysis in an acid medium was found to yield the related photohydroxylation products, in a regioselective process, in addition to the isoquinoline deoxygenated precursor. Photoinduced electron transfer from the donor phenols to the protonated form of the first excited singlet state (S_1) of the pendant isoquinoline *N*-oxide acting as acceptor leads to a red-shifted emissive charge transfer (CT) state that is in fact a radical/cation-radical pair. Homolysis of the N–OH bond restores the aromatic isoquinoline nucleus and produces a hydroxyl radical that can couple to the required ring carbon in the phenol cation-radical to give the photohydroxylation products in a regioselective process controlled by the spin density of the phenol cation-radical. These photohydroxylation processes efficiently compete with the reported tendency to deprotonation in phenol cation-radicals. The photohydroxylation process by itself, and its regioselectivity, exclude a proton-coupled electron transfer mechanism or a consecutive electron transfer/deprotonation reaction. By contrast, the phenol cation-radical exists long enough to undergo the hydroxyl radical coupling reaction that leads to the photohydroxylation products.

1. Introduction

Hydroxyl radicals cause cell damage when generated in excess amounts or if the cellular antioxidant defense is impaired. Also, free iron levels are known to play a crucial role in initiating and catalyzing a variety of radical reactions in the presence of oxygen.[1,2] Aromatic hydroxylation is an important metabolic process, as shown by the reaction of heme-containing P450 flavin monooxygenases, pterin-dependent nonheme monooxygenases, nonheme mononuclear iron dioxygenases and diiron hydroxylases.[3] These enzymes are involved in a number of vital processes such as biosynthesis, degradation of xenobiotics, carcinogenesis and drug metabolism.[4] The rate and selectivity for substrate oxidation is determined jointly by steric effects[5] at the enzyme active site and by intrinsic electronic reactivity.[6] Depending on the particular substrate and the enzyme specificity, the choice of substrates and hydroxylation sites may be dictated by either orientation effects at the binding site or chemical reactivity at the different positions in the substrates. Although experimental evidence for the presence of superoxide in these enzyme mediated reactions exists,[7] the iron-oxene intermediate may act directly in a single oxygen insertion into the substrate following cleavage of the dioxygen bond.[8] The whole mechanism of oxygen insertion into substrates is an area of considerable debate.[9] Although hard experimental evidence is difficult to obtain, the formation of an active oxygen intermediate consisting of a single oxygen atom is a likely pathway for enabling direct oxygen insertion into most known substrates;[6] mechanistic schemes involving peroxy species can also be formulated in some instances, however.[10]

Highly reactive hydroxyl radicals can attack a variety of targets such as lipids, fats and proteins; also, they are involved in a number of major degenerative diseases including aging.[11] Thus, hydroxyl radicals attack the amino acid phenylalanine or salicylate to give, under physiological conditions, *ortho*-, *meta*- and *para*-tyrosines, or 2,3- and 2,5-dihydroxybenzoates, respectively.[12] These nonenzymatic reactions have no control over the position of the highly reactive hydroxyl radical attack on the aromatic ring, so a mixture of almost every possible hydroxylated isomer is usually obtained. These processes commonly involve a reaction between the free hydroxyl radical and

Keywords: Photochemical electron transfer; Radical aromatic hydroxylation.
* Corresponding author. Tel.: +34 952 13 7565; fax: +34 952 13 1941; e-mail: inestrosa@uma.es

0040–4020/$ - see front matter © 2006 Elsevier Ltd. All rights reserved.
doi:10.1016/j.tet.2006.01.003

the intact aromatic ring. However, we recently showed that the reaction between free hydroxyl radicals and methoxy substituted aromatic cation-radicals exhibits these well-defined chemical structures for hydroxyl radical attack to form a new C–OH bond and is an efficient process that is regiochemically controlled by the spin density of the cation-radical.[13]

The ability to include hydroxyl groups rather than methoxy groups as substituents on the aromatic ring has enabled the obtainment of the corresponding phenol cation-radicals. Studying the photochemistry of the acceptor-spacer-donor (AsD) systems designed by the authors, where the acceptor is an isoquinoline *N*-oxide nucleus, the spacer a methylene bridge and the donor a variably substituted phenol, may allow one to describe the oxidation of phenols via PET to a pendant protonated isoquinoline *N*-oxide electron acceptor as a model for the oxidation of phenols, a prototype for these types of electron and proton transfer reactions, and a model for the hydroxylation of phenols. Unlike methoxy substituted donors, the oxidation of phenols should result in a pK_a shift of more than 12 units[14] and no longer rely on its phenolic protons. The electron transfer must thus be coupled to deprotonation and may occur either as a consecutive electron transfer/deprotonation reaction or as a single, concerted, reaction step. This paper reports our results for the PET from phenol donors of compounds **1**, **3** and **5** to bridged protonated isoquinoline *N*-oxide and compares them with those for the previously studied methoxylated derivatives **2** and **4**.

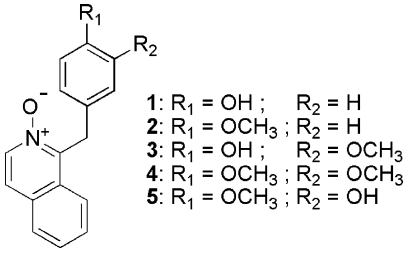

2. Results and discussion

2.1. Photochemical reactivity

Excitation of the protonated forms of the isoquinoline *N*-oxides to the corresponding first excited singlet state S_1 showed electron transfers from donors to produce a charge transfer (CT) state and the resulting radical/cation-radical pair to evolve to hydroxylation of the donor moiety.[13] In parallel, *isc* to the corresponding triplet state T_1 led to the corresponding deoxygenated material. Thus, photolysis of compound **1** (Scheme 1), having a hydroxy substituent in the donor moiety, in CH_2Cl_2/0.1 M TFA led to the corresponding hydroxylated compound **6** (an *ortho*-diphenol) in 21% yield in addition to 50% of the corresponding deoxygenated compound **7**. No other photohydroxylated material was detected.

In order to expand our knowledge of the radical scavenging mechanism in our photochemical process, we studied the

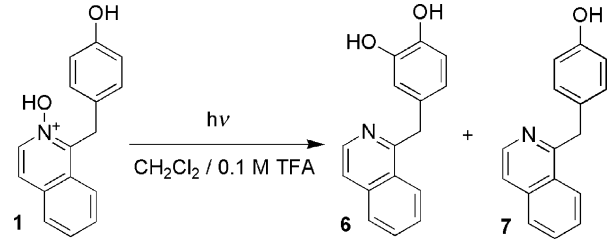

Scheme 1.

influence of various substituents and of the position of the hydroxyl group in some related phenol donors in the AsD system. To this end, we synthesized and photolyzed compound **3**, having a methoxy group *ortho* to the phenol in the donor moiety. Photolysis under identical experimental conditions gave a mixture of the hydroxylated compounds **8** and **9** (48% total hydroxylation yield: 35% of **8** and 13% of **9**; **8/9**=2.7/1) plus the related deoxygenated compound **10** (28%) (Scheme 2).

Irradiation of the isomeric compound **5** gave a similar result to that for compound **3**. The exchange of methoxyl and hydroxyl substituents altered neither the balanced yield nor the regioselectivity of the photochemical reaction. Photolysis of **5** yielded a mixture of the hydroxylated compounds **11** and **12** (45% total hydroxylation yield: 30% of **11** and 15% of **12**; **11/12**=3/1) plus the related deoxygenated compound **13** (32%) (Scheme 3). Therefore, the photolysis of the isomeric compounds **3** and **5** provided comparable yields of hydroxylated (**11** and **12**) and deoxygenated (**13**) material, and resulted in similar regioselectivity in the hydroxylation process.

2.2. Influence of the photoreaction conditions

In order to gain additional knowledge about the photoreaction mechanism and the influence of the conditions on the outcome, we photolysed compound **1** using the same TFA concentration as previously (0.1 M), but water as solvent. The outcome of the photoreaction was identical, and only compound **6** and **7** were detected, in the same relative proportion. The only change worth noting was a relative decrease in the reaction rate resulting from the need for longer irradiation timers in order to obtain similar conversion levels. Similarly, the photoloysis of compound **3** in water exhibited no change in the deoxygenated/hydroxylated ratio—only a similar decrease in reaction rate was observed now—, nor in the **8/9** photohydroxylated regioisomer ratio. This compound was also photolysed in 0.1 M trifluoromethanesulfonic acid in water (i.e., in a more acidic medium by ca. 13 pK_a units), the reaction profile and yields remaining unaltered.

2.3. Fluorescence

From the data in Table 1 it follows that all the compounds discussed here exhibit a dual fluorescence emission that is related to the LE emission on excitation at a short wavelength (λ_{exc} 330 nm), and a CT emission on excitation at a long wavelength (λ_{exc}=360 nm). The LE emission is a common emission band because all studied compounds possess the same acceptor (viz. the isoquinoline *N*-oxide).

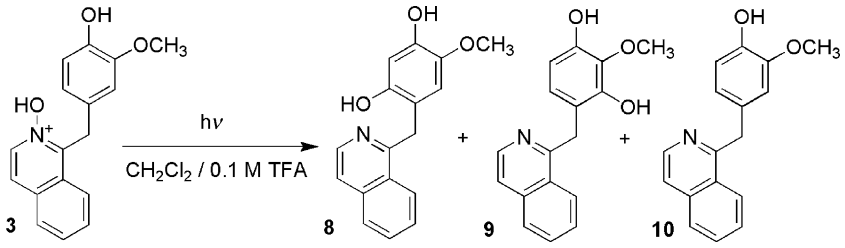

Scheme 2.

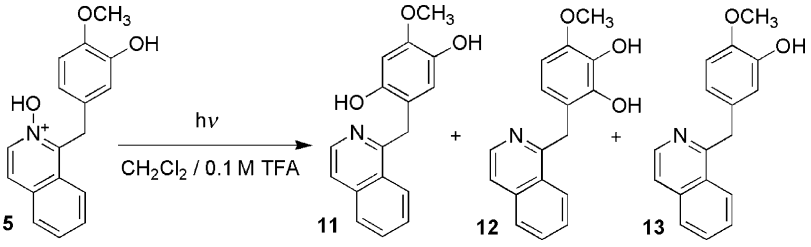

Scheme 3.

Table 1. Fluorescence spectroscopy data: dichloromethane 0.1 M TFA

Compound	λ_{fl} (ϕ)[a]	
	λ_{exc} 330 (nm)[b]	λ_{exc} 366 (nm)[c]
1	386 (1.0×10^{-3})	480 (4.3×10^{-2})
2[d]	380 (2.0×10^{-3})	479 (2.0×10^{-2})
3	382 (4.0×10^{-4})	497 (2.0×10^{-2})
4[d]	382 (4.0×10^{-3})	500 (5.4×10^{-2})

[a] Emission maximum (nm).
[b] Emission corresponding to the protonated locally excited (LE) state.
[c] Emission corresponding to the charge transfer (CT) state.
[d] Data from Ref. 13.

The CT emission appears at the same wavelength for the monosubstituted compounds **1** and **2**; this suggests that the CT state of these monosubstituted donor compounds is in the same energy situation and possess similar fluorescence quantum yields. This is a result of the electron-transfer process producing an equivalent CT state for phenol and methoxy substituted donor compounds.

This situation is also observed in the disubstituted compounds **3**, **4** and **5**. The dimethoxy substituted compound **4**, and the monomethoxy–monohydroxy substituted homologs **3** and **5**, exhibit the CT state emission at the same energy level (emissions around 500 nm), red shifted with respect to the monosubstituted **1** and **2** by effect of their ability to act as donors. However, the only variable that alters the CT state wavelength emission is the number of oxa substituents on the donor ring—not the quality as methoxyl or hydroxyl groups—; therefore, the CT states of the related phenol cation-radicals are homologous to the methoxy derivatives and the photohydroxylation reaction occurs as a result.

2.4. Mechanistic considerations

The outcome of the photolysis of the studied compounds reveals that the coupling of the hydroxyl radical to the phenol cation-radical is a regioselective process. The preferred positions for the coupling of the hydroxyl radical over the phenol cation-radical are consistent with the reported positions in the aromatic moiety. As shown in Scheme 4, the mechanism for the photochemical hydroxylation of aryls by excitation of the protonated isoquinoline *N*-oxide can be interpreted as a stepwise process in which the photoinduced electron transfer produces a hydroxyl radical that subsequently couples with the cation-radical of the aryl to form a new C–OH bond. As a result, the spin density of the transient phenol cation-radical will dictate the final hydroxylation position in the overall photoreaction.

We can thus assume a mechanism similar to that reported for the photohydroxylation in the related compound **2** (Scheme 4; ET) to operate for the hydroxy substituted compound **1** as well. In this way, electron transfer from the phenol moiety to the first excited singlet state S_1 of the acceptor, the protonated form of the isoquinoline *N*-oxide **1**, will produce a CT state $\mathbf{14_H}$ that will in fact be a radical/cation-radical pair. Homolytic N–OH bond cleavage results in rearomatization of the isoquinoline nucleus to give the cation-radical $\mathbf{15_H}$ and release the hydroxyl radical. The cation $\mathbf{16_H}$ loses a proton to rearomatize the donor moiety and give the hydroxylated diphenol **6**.

Based on the proposed mechanism (Scheme 4; ET), the driving force that determines the regioselective hydroxylation site is related with the spin density in the transient phenol cation-radical (see Section 4). The spin density in $\mathbf{14_H}$ is highest in the *ortho* position to the phenol group and lowest in the *meta* position. Therefore, the experimental regiocontrol exhibited by the photochemical reaction of **1** is consistent with this assumption.

Although only a few experiments have been conducted to determine the pK_a values[15] or lifetimes of phenolic cation-radicals,[16] nonpolar solvents have provided a convenient way of producing cation-radicals from a variety of solutes via ET.[17] However, the phenol cation-radical is subsequently deprotonated in a process that is subject to a

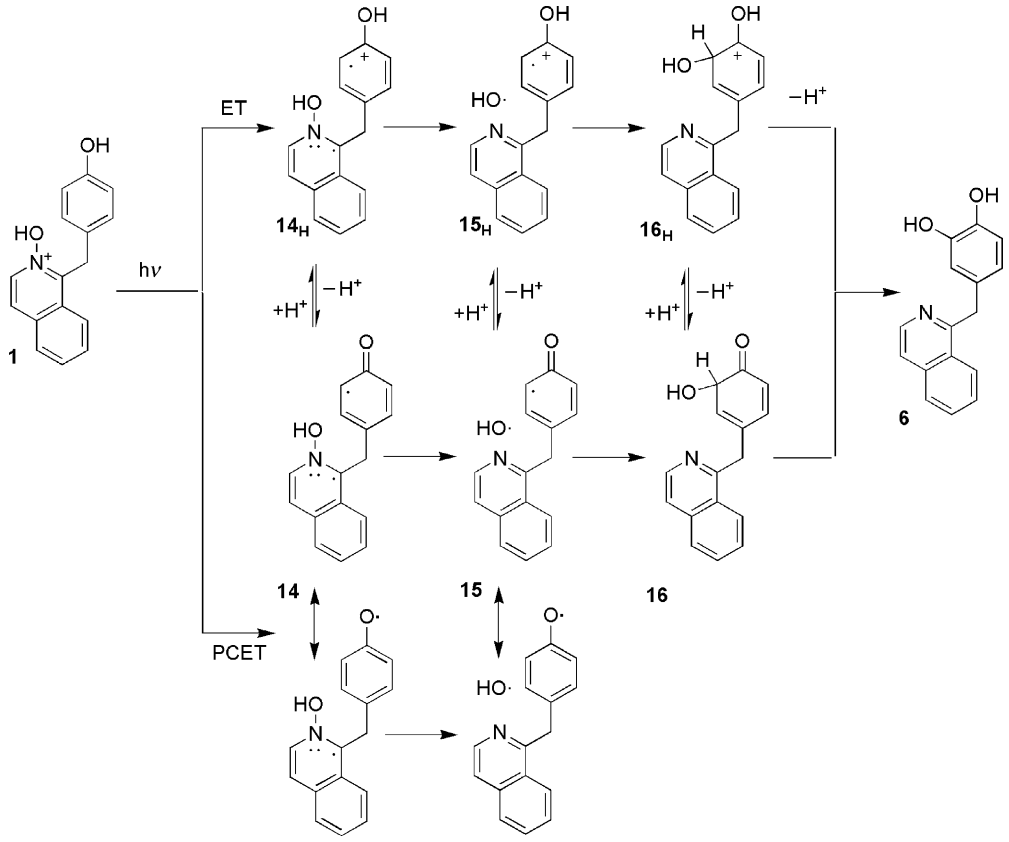

Scheme 4.

very low energy barrier[18] and yields the phenoxyl radical as a result of the markedly increased acidity order of the phenol cation-radical relative to neutral phenols. Therefore, one must consider the possibility of the transient intermediates $\mathbf{14_H}$–$\mathbf{16_H}$ donor cationic species being deprotonated to the corresponding donor radicals **14**–**16** in a proton coupled electron transfer mechanism (Scheme 4, PCET). However, the keto form of these intermediates concentrates the spin density at the same position in the donor ring as the corresponding protonated forms $\mathbf{14_H}$–$\mathbf{16_H}$ and the regioselectivity for hydroxyl coupling remains unchanged as a result. Although an equilibrium between the protonated or keto form of the deprotonated intermediates in the reaction medium is possible, both species induce the same regiocontrol over the hydroxylation process as they result in the same location for the highest spin densities in the donor ring. Therefore, bond formation in the hydroxylation process can occur over the protonated or deprotonated form of the phenol donor cation-radical.

2.4.1. Does the deprotonation of the phenol cation-radical precede the radical coupling reaction? If the deprotonation of the phenol cation-radical were the main reaction pathway for these transient intermediates, then the resulting radicals, (e.g., **14** or **15** in Scheme 4) would be better defined as phenoxy radicals than as carbon centered radicals. Oxygen centered radicals (e.g., $ArO^{\cdot}$) do not react with hydroxyl radical to form a peroxy derivative as this process is endoergonic,[19] so only the carbon centered radicals can give the observed hydroxylation products. Therefore, deprotonation of the corresponding phenol cation-radicals leading to phenoxyl radicals[18] need not be the main pathway for our compounds, even though this phenomenon has been extensively studied and postulated as the main pathway for phenol cation-radical intermediates. The possibility of the proton coupled electron-transfer mechanism reported for phenols[20] directly yielding the phenoxyl radical and hence inhibiting the hydroxylation process as an alternative to this stepwise mechanism can therefore be discarded.

From the photoreaction of **3** one may conclude that the presence of the methoxy group on the aromatic donor ring strongly influences the outcome of the hydroxylation process. The hydroxylation position in the donor ring changes from that nearest to the phenol group to the two possible *meta* sites (**8** and **9**) and the ratio of hydroxylation to deoxygenation products increases as a result. This is consistent with our hypothesized PET pathway from the donor to the S_1 state of the acceptor, which is favored by an increased electron donor ability. The regiochemistry of the hydroxylation reaction is now consistent with that previously reported for the parent compound **4** having two methoxy groups instead of the monomethoxy–monohydroxyl derivative **3**. Because the hydroxyl-radical coupling can occur over the donor phenol cation-radical before the proton is lost, the calculated spin densities are consistent with the preferred orientation of hydroxylation also observed in the parent compound **4**. However, if the deprotonation of the donor phenol cation-radical occurs before the hydroxyl-radical coupling, the unpaired electron in the resulting keto-radical (Scheme 5) will be in a ring

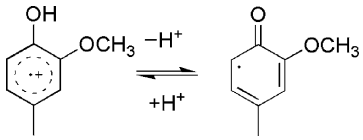

Scheme 5.

position inconsistent with the photohydroxylation products obtained (**8** and **9**). Therefore, the phenol cation-radical must be the intermediate responsible for the formation of **8** and **9**, and hence for the corresponding deprotonated species not forming.

Two different configurations can be formulated for the disubstituted cation-radicals resulting from **3** and **5** (Scheme 6). The cation-radial formed in the electron-transfer process of **3** (a, Scheme 6) can be described as the two limiting cations-radicals **a1** and **a2**. While all resonant forms resulting from cation-radical **a1** can only undergo hydroxylation by hydroxyl-radical/carbon-centered radical coupling on the ring *meta*-position (with respect to the methylene bridge; empty arrow), the corresponding cation-radical **a2** localizes the radical density at appropriate positions (black arrows), which is quite consistent with the regioselectivity observed in the photohydroxylation process.

Thus, the preferred charge density is located over the methoxyl-substituted carbon instead of the hydroxyl-substituted one, which hinders deprotonation and favors photohydroxylation.

However, in the isomeric cation-radical formed from compound **5** (b, Scheme 6), the cation-radical **b2**, which locates the positive charge over the hydroxyl substituted carbon, is the resonant form that correlates well with the observed photohydroxylation positions. Because the hydroxylation products obtained in the photolysis of **5** have the phenol group in *ortho* with respect to the methylene bridge, the positive charge must be localized in the same relative position as in **a2**, which allows high spin densities to be concentrated at appropriate carbon atoms in the aromatic ring.

The charge and unpaired electron densities distributions for various substituted phenols and the corresponding methoxyl derivatives have been widely discussed in relation to SN2Ar* and radical processes in the literature.[21] The directing influence of the electron-donor susbstituents can be rationalized in terms of the calculated values for cation-radicals. The B3LYP/6-31g(d,p) electronic spin densities for 4-methyl phenol, 2-methoxy-4-methyl phenol and 2-methoxy-3-methyl phenol cations-radicals as model molecules were calculated and the resulting values found to be consistent with their experimental counterparts (i.e., with the encounter hydroxylation positions).[22]

2.4.2. π-Electron versus oxygen centred electron transfer mechanisms. Intermolecular electron-transfer reactions from phenols to selected acceptors have been studied and direct, synchronous formation of phenoxyl radicals and phenol cation-radicals in nearly the same relative amounts observed in all cases (Scheme 7).[16b,23] This was ascribed to two competing electron-transfer channels depending on the geometry of encounter between the parent acceptor and the phenol molecule. The electron transfer was found to occur via two different pathways synchronously generating the phenol cation-radical ($ArOH^{+\cdot}$) and phenoxyl radicals ($ArO^{\cdot}$). The proportion of the fast formation of the two transients by electron-transfer can be expected to be about 50% for each reaction channel. This means that both pathways have the same probability.

Thus, intermolecular electron-transfer from the aromatic ring to the acceptor occurs, the positive charge being stabilized within the aromatic system with the assistance of substituents of the ring. The other type of attack involves an interaction between the phenolic oxygen atom and the acceptor,

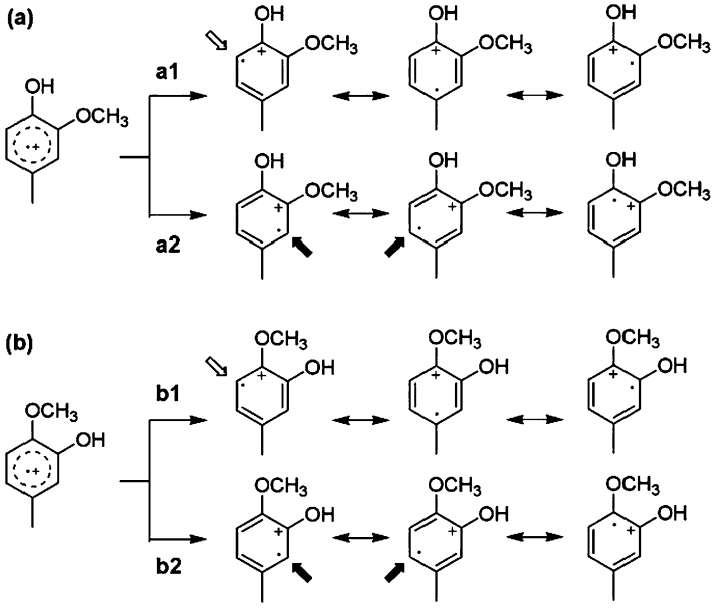

Scheme 6.

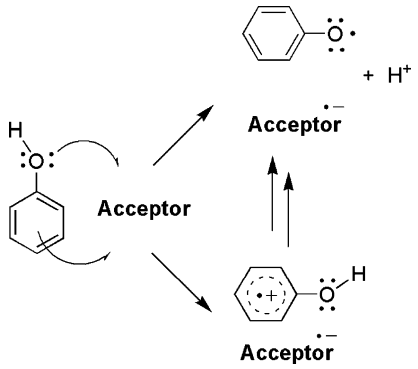

Scheme 7.

immediately followed by deprotonation, the products being phenoxyl radicals. Obviously, this intermolecular reaction can take place via two different channels involving encounters between the parent ions and the aromatic ring, as well as the hydroxyl group in the solute molecule. Hence, such different encounter situations lead to the synchronous formation of the phenol cation-radical and phenoxyl radicals. Two different types of products can therefore be obtained depending on the particular intermolecular encounter geometry.[16b,24]

When the phenols and the acceptor moieties are covalently bridged, as was the case in our intramolecular situation, the encounter geometries for the electron-transfer are restricted by the short methylene chain. In this situation, restricted geometries can govern the reaction pathways. In compounds **1**, **3** and **5**, the hydroxyl groups in the aromatic donors are faraway oriented with respect to the protonated isoquinoline *N*-oxide acceptor, so, based on the previous argument, intramolecular electron-transfer from the aromatic ring to the acceptor, leading to the phenol cation-radical, will occur instead of direct electron transfer from the phenolic oxygen atom, which will follow immediate deprotonation with the production of phenoxyl radicals. In this way, a carbon centered radical capable of reacting with the hydroxyl radical that can give the photohydroxylation products is obtained. Rapid generation of the cation-radicals and their delayed deprotonation into radicals can occur in all cases studied in nonpolar solvents. Studies have shown that, even though the cation-radicals are deprotonated, they are stable enough to be characterized in dry solvents at room temperature. This mechanism is supported by the photochemical reaction of the isomeric compound **17**, for which no photohydroxylation product was detected; the sole product obtained was the corresponding deoxygenated compound **18**, in 85% yield (Scheme 8). Here, the encounter geometry can determine the characteristics of the electron transfer product.[24]

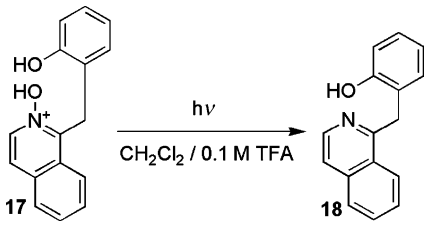

Scheme 8.

Hence, the proximity of the hydroxyl group of the phenol in **17** to the acceptor can be assumed to result in a preferred electron transfer from the phenolic oxygen atom directly leading to the phenoxyl radical—which cannot couple with the hydroxyl radical—, the photohydroxylation process being inhibited as a result. Based on these results, we can assume the presence of two structures strongly differing in their tendency to rapid dissociation after ionization: whereas the oxygen-localized cation-radical dissociates immediately to a phenoxyl-radical, the delocalized planar cation-radical is a metastable species on a timescale of a few 100 ns.[23b] Subsequently, it can be deprotonated more slowly—albeit before it can undergo hydroxyl radical coupling to give the photohydroxylation products.

This reflects in the fact that, the charge and spin densities in the direct electron transfer from the aromatic ring to the protonated isoquinoline *N*-oxide acceptor to give the corresponding donor cation-radical are strongly influenced by the position of the oxa-substituents; however, they have no decisive influence on the quality of homologous substituents such as hydroxyl/methoxyl groups. On the other hand, the resulting cation-radical possesses a long enough lifetime to allow the radical to couple and produce the hydroxylated material prior to deprotonation.

3. Conclusions

The photolysis of a protonated isoquinoline *N*-oxide covalently bonded to a substituted phenol gives the corresponding hydroxylated diphenol derivatives with absolute regiocontrol over the hydroxylation position of the starting phenols. Our proposed electron transfer-initiated photohydroxylation mechanism is also feasible for these phenol derivatives if one excludes the commonly accepted PCET and sequential electron transfer/deprotonation reactions. The ET from the donor phenol ring to the protonated isoquinoline *N*-oxide involves the simultaneous formation of a hydroxyl radical and the phenol cation-radical, which undergo hydroxyl coupling before deprotonation to give the photohydroxylated material. Because the hydroxyl radical and the phenol cation-radical are simultaneously produced, the radical coupling reaction takes complete regiocontrol over the ring hydroxylation process. The photohydroxylation process produced by isoquinoline *N*-oxide photochemistry is effective enough to compete with the deprotonation process put forward for phenol cation-radicals.

4. Experimental

Material and equipment. All reagents were used as received. The solvents for absorption and fluorescence measurements were spectrophotometric grade and used without further purification. HRMS are reported as *m*/*z*. ^{1}H and ^{13}C NMR spectra (200 and 50 MHz, respectively) were recorded from $CDCl_3$ solutions, using the solvent residual proton signal as standard. TLC analyses were performed on silica gel 60 F 256 plates and column chromatography was carried out on silica gel 60 (70–230 mesh). Melting points were obtained in open capillaries and are given uncorrected.

Spectroscopic studies. Samples for recording UV/vis and fluorescence emission spectra were prepared in spectroscopic grade solvents and adjusted to a linear grade response. Fluorescence quantum yields were determined by comparison with quinine sulfate and corrected for the refractive index of the solvent.

4.1. Synthesis of 1-(4-hydroxybenzyl)isoquinoline *N*-oxide (1)

4.1.1. 4-Tosyloxy-benzaldehyde (19).[25] A mixture of 50 mL of dichloromethane and 20 mL of a 30% aqueous solution of NaOH was vigorously stirred, and 1.59 g (13 mmol) of 4-hydroxybenzaldehyde and 200 mg of TEBA added under nitrogen atmosphere. A solution of tosyl chloride containing 4.34 g (21 mmol) in 50 mL of dichloromethane was then added dropwise and the reaction mixture stirred for 6 h. The organic phase was washed with water (2×50 mL), dried and concentrated. The crude product was pure enough for use without further purification in the next step. White solid; mp=72–73 °C (hexane); yield 82%; ^{1}H NMR ($CDCl_3$) δ 2.43 (s, 3H,), 7.15 (d, 2H, J=9.1 Hz), 7.30 (d, 2H, J=8.5 Hz), 7.70 (d, 2H, J=8.5 Hz), 7.81 (d, 2H, J=8.6 Hz), 9.95 (s, 1H); ^{13}C NMR ($CDCl_3$) δ 21.4, 122.7, 128.1, 129.8, 131.0, 131.7, 134.6, 145.7, 153.5, 190.4; MS *m*/*z* (%) 276 (4) $[M]^+$, 155 (25), 91 (100), 65 (72). Anal. Calcd for $C_{14}H_{12}O_4S$: C, 60.86; H, 4.38. Found: C, 60.88; H, 4.40.

4.1.2. 4-Tosyloxy-benzylalcohol (20).[26] A solution of 4-tosyloxy-benzaldehyde containing 3.04 g (11 mmol) in MeOH (50 mL) was supplied with 0.416 g (11 mmol) of $NaBH_4$ at 0 °C in four portions. After stirring for 5 h, water was added to the reaction mixture and the resulting product extracted with CH_2Cl_2, dried over $MgSO_4$ and evaporated to obtain the protected benzyl alcohol. Oil; yield 78%; ^{1}H NMR ($CDCl_3$) δ 2.42 (s, 3H), 4.61 (s, 2H), 6.93 (d, 2H, J=8.5 Hz), 7.22–7.67 (m 4H), 7.67 (d, 2H, J=8.5 Hz); ^{13}C NMR ($CDCl_3$) δ 21.0, 63.5, 121.6, 127.3, 127.7, 129.1, 139.2, 144.7, 148.1; MS *m*/*z* (%) 278 (6) $[M]^+$, 155 (24), 107 (11), 106, (100), 91 (100), 65 (64). Anal. Calcd for $C_{14}H_{14}O_4S$: C, 60.42; H, 5.07. Found: C, 60.40; H, 5.10.

4.1.3. 4-Tosyloxy-benzylchloride (21).[26] A round-bottom flask containing 1.67 g (6 mmol) of 4-tosyloxy-benzyl-alcohol was cooled in a water–ice mixture and supplied with $SOCl_2$ (0.5 mL; 7 mmol) via a dropping funnel. The reaction mixture was heated in a water bath for 6 h. Excess $SOCl_2$ was then removed in vacuo and the residue dissolved in CH_2Cl_2 (200 mL), washed with water (3×50 mL), dried and concentrated. White solid; mp=80–82 °C (hexane); yield 88%; ^{1}H NMR ($CDCl_3$) δ 2.43 (s, 3H), 4.51 (s, 2H), 6.95 (d, 2H, J=8.5 Hz), 7.27–7.31 (m, 4H), 7.67 (d, 2H, J=8.5 Hz); ^{13}C NMR ($CDCl_3$) δ 21.5, 45.0, 122.5, 128.3, 129.7, 132.1, 136.3, 145.4, 149.3; MS *m*/*z* (%) 298 (2) $[M^+ + 2]$, 296 (4) $[M]^+$, 155 (33), 106, (50), 91 (100), 65 (46). Anal. Calcd for $C_{14}H_{13}ClO_3S$: C, 56.66; H, 4.42. Found: C, 56.67; H, 4.45.

4.1.4. 4-Hydroxybenzyl isoquinoline (7).[27] In a 100 mL two-necked flask were placed 1 g (3.3 mmol) of 4-tosyloxy-benzylchloride, isoquinoline Reissert (0.73 g; 2.8 mmol) and TEBA (200 mg) in 20 mL of benzene under an argon atmosphere. The resulting mixture was vigorously stirred and a solution of 50% aqueous NaOH (10 mL) was added. After stirring at room temperature for 24 h, the organic layer was collected, washed with water, dried and concentrated to obtain a residue that was subsequently hydrolyzed.

The crude residue was dissolved in a mixture of 5 mL of methanol and 10 mL of 20% aqueous NaOH, the resulting solution being refluxed for 3 h. Once cool, the solution was extracted with CH_2Cl_2 (3×100 mL). The organic extracts were dried with $MgSO_4$, the solvent being removed in vacuo. The product was purified by column chromatography. Yellow solid; yield 72%; ^{1}H NMR ($CDCl_3$) δ 4.57 (s, 2H,), 6.63 (d, 2H, J=8.5 Hz), 7.03 (d, 2H, J=8.5 Hz), 7.49–7.57 (m, 2H), 7.64 (t, 1H, J=6.7 Hz), 7.80 (d, 1H, J=8.5 Hz), 8.16 (d, 1H, J=7.9 Hz), 8.45 (d, 1H, J=5.5 Hz); ^{13}C NMR ($CDCl_3$) δ 40.4, 115.2, 120.1, 125.9, 126.9, 127.1, 127.3, 129.2, 129.8, 130.1, 136.5, 140.5, 155.0, 160.4; MS *m*/*z* (%) 236 (4) $[M]^+$, 235 (33), 234 (100), 233 (19), 204 (15), 75 (36). Anal. Calcd for $C_{16}H_{13}NO$: C, 81.68; H, 5.57; N, 5.95. Found: C, 81.76; H, 5.85; N, 5.97.

4.1.5. 1-(4-Hydroxybenzyl)isoquinoline *N*-oxide (1). To a solution of 4-hydroxybenzyl isoquinoline (0.8 g; 3.4 mmol) in 25 mL of chloroform, MCPBa (0.828 g; 4.8 mmol) was added and the resulting solution stirred at room temperature for 24 h. The solution was washed with saturated aqueous $NaHCO_3$ and water, dried and concentrated, the resulting solid being recrystalized from AcOEt. Brown solid; mp=203–204 °C (AcOEt); yield 83%; ^{1}H NMR ($CDCl_3$) δ 4.69 (s, 2H), 6.57 (d, 2H, J=8.5 Hz), 7.05 (d, 2H, J=8.5 Hz), 7.54–7.68 (m, 3H), 7.78 (d, 1H, J=8.5 Hz), 8.03 (d, 1H, J=7.9 Hz), 8.21 (d, 1H, J=7.3 Hz); ^{13}C NMR ($CDCl_3$) δ 30.5, 115.1, 122.9, 124.4, 126.9, 127.2, 128.2, 129.2, 129.4, 129.9, 135.4, 148.3, 155.3; MS *m*/*z* (%) 251 (34) $[M]^+$, 234 (100), 204 (43). Anal. Calcd for $C_{16}H_{13}NO_2$: C, 76.48; H, 5.21; N, 5.57. Found: C, 76.21; H, 5.28; N, 5.80.

4.2. Synthesis of 1-(3-methoxy-4-hydroxybenzyl)isoquinoline *N*-oxide (3)

4.2.1. 3-Methoxy-4-tosyloxy-benzaldehyde (22).[28] Prepared by using the above-described procedure for **19**. White solid; mp=116–117 °C (hexane); yield 85%; ^{1}H NMR ($CDCl_3$) δ 2.44 (s, 3H), 3.63 (s, 3H), 7.25–7.44 (m, 5H), 7.75 (d, 2H, J=7.9 Hz), 9.91 (s, 1H); ^{13}C NMR ($CDCl_3$) δ 21.6, 55.7, 111.1, 124.1, 128.4, 129.4, 132.9, 135.7, 142.9, 145.4, 152.5, 190.7; MS *m*/*z* (%) 306 (2) $[M]^+$, 155 (34), 91 (100), 65 (69). Anal. Calcd for $C_{15}H_{14}O_5S$: C, 58.81; H, 4.61. Found: C, 58.83; H, 4.64.

4.2.2. 3-Methoxy-4-tosysloxy-benzylalcohol (23).[28] Prepared by using the above-described procedure for **20**. White solid; mp=90–91 °C (AcOEt); yield 90%; ^{1}H NMR ($CDCl_3$) δ 1.97 (t, 1H, J=4.9 Hz), 2.43 (s, 3H), 3.51 (s, 3H), 4.62 (s, 2H), 6.80–6.87 (m, 2H), 7.08 (d, 1H, J=8.5 Hz), 7.28 (d, 2H, J=7.9 Hz), 7.73 (d, 2H, J=7.3 Hz); ^{13}C NMR ($CDCl_3$) δ 21.5, 55.4, 64.4, 111.0, 118.5, 123.7, 128.5, 129.3, 133.1, 137.4, 141.2, 145.0, 151.7; MS *m*/*z* (%) 308 (3) $[M]^+$, 155 (17), 91 (100), 65 (47). Anal. Calcd for $C_{15}H_{16}O_5S$: C, 58.43; H, 5.23. Found: C, 58.46; H, 5.24.

4.2.3. 3-Methoxy-4-tosysloxy-benzylchloride (24). Prepared by using the above-described procedure for **21**. White solid; mp=110–112 °C (AcOEt); yield 86%; ^{1}H NMR ($CDCl_3$) δ 2.43 (s, 3H), 3.57 (s, 3H), 4.50 (s, 2H), 6.85–6.89 (m, 2H), 7.08 (d, 1H, J=9.1 Hz), 7.28 (d, 2H, J=7.9 Hz), 7.74 (d, 2H, J=7.9 Hz); ^{13}C NMR ($CDCl_3$) δ 21.5, 45.5, 55.5, 112.8, 120.5, 123.9, 128.4, 129.3, 133.0, 137.4, 138.1, 145.1, 151.8; MS m/z (%) 326 (6) $[M]^+$, 91 (100), 65 (66). Anal. Calcd for $C_{15}H_{15}O_4ClS$: C, 55.13; H, 4.63. Found: C, 55.14; H, 4.65.

4.2.4. 1-(3-Methoxy-4-hydroxybenzyl)isoquinoline (10). Prepared by using the above-described procedure for **7**. White solid; mp=139–140 °C (AcOEt); yield 73%; ^{1}H NMR ($CDCl_3$) δ 3.70 (s, 3H), 4.57 (s, 2H), 6.77–6.79 (m, 3H), 7.48–7.59 (m, 3H), 7.79 (d, 1H, J=8.5 Hz), 8.16 (d, 1H, J=8.5 Hz), 8.47 (d, 1H, J=6.1 Hz); ^{13}C NMR ($CDCl_3$) δ 41.6, 55.7, 111.3, 114.4, 119.8, 121.3, 125.8, 127.1, 127.3, 129.2, 129.9, 131.2, 136.6, 141.8, 144.2, 146.7, 160.4; MS m/z (%). Anal. Calcd for $C_{17}H_{15}NO_2$: C, 76.96; H, 5.70; N, 5.28. Found: C, 76.98; H, 5.73; N, 5.29.

4.2.5. 1-(3-Methoxy-4-hydroxybenzyl)isoquinoline *N*-oxide (3). An amount of 0.8 g (3.0 mmol) of 1-(3-methoxy-4-hydroxybenzyl)isoquinoline was reacted as for the preparation of **1**. White solid; mp=204–205 °C (AcOEt); yield 73%; ^{1}H NMR ($CDCl_3$) δ 3.81 (s, 3H), 4.55 (s, 2H), 5.60 (s, 1H), 6.74 (s, 2H), 7.04 (s, 1H), 7.50–7.64 (m, 3H), 7.76 (d, 1H, J=7.9 Hz), 8.02 (d, 1H, J=7.9 Hz), 8.20 (d, 1H, J=6.7 Hz); ^{13}C NMR ($CDCl_3$) δ 31.2, 55.8, 111.9, 114.6, 120.5, 121.0, 122.5, 124.1, 127.3, 128.7, 129.2, 129.3, 136.6, 144.7, 147.0, 147.5; MS m/z (%) 281 (13) $[M]^+$, 280 (20), 264 (100). Anal. Calcd for $C_{17}H_{15}NO_3$: C, 76.96; H, 5.70; N, 5.28. Found: C, 76.99; H, 5.73; N, 5.30.

4.2.6. 1-(3-Hydroxy-4-methoxybenzyl)isoquinoline *N*-oxide (5). An amount of 0.75 g (2.8 mmol) of 1-(3-hydroxy-4-methoxybenzyl)isoquinoline[13] was reacted as for the preparation of **1**. Brown solid; mp=195–196 °C (AcOEt); yield 73%; ^{1}H NMR ($CDCl_3$): δ 3.79 (s, 3H, $-OCH_3$), 4.71 (s, 2H, $-CH_2-$), 5.65 (s, 1H, OH), 6.71 (d, 1H, J=7.9 Hz, $H_{5'}$), 6.80–6.86 (m, 2H, $H_{2'}$, $H_{6'}$), 7.50–7.65 (m, 3H, H_4, H_6, H_7), 7.76 (d, 1H, J=8.2 Hz), 7.99 (d, 1H, J=8.5 Hz, H_8), 8.22 (d, 1H, J=7.3 Hz, H_3); ^{13}C NMR ($CDCl_3$): δ 30.6, 55.4, 111.4, 115.0, 119.4, 120.3, 122.9, 124.2, 124.4, 127.2, 128.3, 129.1, 129.4, 129.8, 135.4, 146.0, 148.1; MS (EI, relative %) 281 (30) $[M]^+$, 280 (60), 264 (100). Anal. Calcd for $C_{17}H_{15}NO_2$ (281.31): C, 76.96; H, 5.70; N, 5.28. Found: C, 76.99; H, 5.72; N, 5.29.

4.2.7. 1-(2-Hydroxybenzyl)isoquinoline *N*-oxide (17).[29]

4.3. General procedure for irradiation of samples

A 10^{-3} M solution of the corresponding *N*-oxide in CH_2Cl_2 and 0.1 M TFA was bubbled with argon and irradiated through Pyrex at room temperature under an Ar atmosphere, using a medium-pressure mercury lamp (150 W) for 10 min. The solutions were then washed with aqueous $NaHCO_3$ and H_2O, and dried over $MgSO_4$. The solvent was evaporated under reduced pressure and the resulting material separated by column chromatography. When necessary, mixtures of regioisomeric phenols were further separated by preparative TLC.

4.3.1. 1-(3,4-Dihydroxybenzyl)isoquinoline (6). See Ref. 30.

4.3.2. 1-(2,4-Dihydroxy-5-methoxybenzyl)isoquinoline (8). Oil; yield 35%; ^{1}H NMR ($CDCl_3$) δ 3.81 (s, 3H), 4.48 (s, 2H), 6.60 (s, 1H), 6.77 (s, 1H), 7.55 (d, 1H, J=6.1 Hz), 7.64–7.76 (m, 2H), 7.83 (d, 1H, J=7.9 Hz), 8.34 (d, 1H, J=6.1 Hz), 8.40 (d, 1H, J=7.3 Hz); ^{13}C NMR ($CDCl_3$) δ 31.2, 55.8, 111.9, 114.6, 120.9, 122.8, 124.3, 127.4, 128.3, 128.6, 128.8, 129.5, 129.6, 136.1, 144.5, 146.9, 147.9; MS m/z (%) 281 (100) $[M]^+$, 168 (72), 167 (79); HRMS (FAB) m/z calcd for $C_{17}H_{15}NO_3$ $(M)^+$281.1052, found 281.1060.

4.3.3. 1-(2,4-Dihydroxy-3-methoxybenzyl)isoquinoline (9). Oil; yield 13%; ^{1}H NMR ($CDCl_3$) δ 3.98 (s, 3H), 4.51 (s, 2H), 6.41 (d, 1H, J=8.5 Hz), 6.91 (d, 1H, J=8.5 Hz), 7.56 (d, 1H, J=5.5 Hz), 7.68–7.76 (m, 2H), 7.83 (d, 1H, J=6.7 Hz), 8.34 (d, 1H, J=6.1 Hz), 8.40 (d, 1H, J=8.5 Hz); ^{13}C NMR ($CDCl_3$) δ 36.2, 57.4, 111.4, 122.7, 123.6, 125.2, 125.8, 126.8, 128.6, 129.0, 131.6, 136.5, 136.6, 140.9, 145.9, 148.1, 158.3; MS m/z (%) 281 (100) $[M]^+$, 168 (72), 167 (79); HRMS (FAB) m/z calcd for $C_{17}H_{15}NO_3$ $(M)^+$281.1052; found 281.1056.

4.3.4. 1-(2,5-Dihydroxy-4-methoxybenzyl)isoquinoline (11). Oil; yield 30%; ^{1}H NMR ($CDCl_3$) δ 3.81 (s, 3H), 4.48 (s, 2H), 6.59 (s, 1H), 6.77 (s, 1H), 7.55 (d, 1H, J=6.5 Hz), 7.20–7.60 (m, 2H), 7.82 (d, 1H, J=6.7 Hz), 8.34 (d, 1H, J=6.1 Hz), 8.40 (d, 1H, J=9.1 Hz); ^{13}C NMR ($CDCl_3$) δ 36.1, 56.2, 101.4, 122.8, 122.9, 125.9, 126.5, 126.9, 128.6, 131.6, 140.9, 144.2, 147.6, 153.6, 156.7; MS m/z (%) 281 (100) $[M]^+$, 280 (72), 167 (79); HRMS (FAB) m/z calcd for $C_{17}H_{15}NO_3$ $(M)^+$281.1052; found 281.1059.

4.3.5. 1-(2,3-Dihydroxy-4-methoxybenzyl)isoquinoline (12). Oil; yield 15%; ^{1}H NMR ($CDCl_3$) δ 3.77 (s, 3H), 4.53 (s, 2H), 6.36 (d, 1H, J=8.5 Hz), 6.91 (d, 1H, J=8.5 Hz), 7.53 (d, 1H, J=5.7 Hz), 7.62–7.69 (m, 2H), 7.79 (d, 1H, J=7.3 Hz), 8.33–8.40 (m, 2H); ^{13}C NMR ($CDCl_3$) δ 36.1, 56.3, 108.2, 122.8, 125.8, 126.5, 126.9, 127.2, 128.5, 131.6, 136.6, 138.5, 141.0, 144.0, 148.1, 157.5; MS m/z (%) 281 (100) $[M]^+$, 168 (72), 167 (79); HRMS (FAB) m/z calcd for $C_{17}H_{15}NO_3$ $(M)^+$: 281.1052; found 281.1057.

4.4. Theoretical calculations

In order to ensure reliable results, density functional theory (DFT) calculations were carried out by using the software Gaussian 98[22a] on an SGI Origin 2000 supercomputer. We used Becke's three-parameter exchange functional in combination with the LYP correlation functional (B3LYP).[22b] The hybrid functional (HF/DFT) B3LYP was previously shown to provide electronic spin densities similar to those obtained from high-level CAS computations with the same basis sets.[22c] We used the 6-31g(d,p) basis set,[22d] which is a split-valence set and includes a series of *d*-polarization functions on heavy atoms and *p*-polarization

functions for the hydrogens. This set provides a compromise between accuracy and applicability to large molecules.

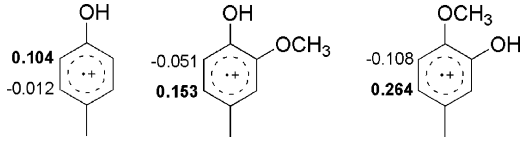

Acknowledgements

The authors acknowledge financial support from Spain's DGI (Projects BQU01-1890 and CTQ04-565). D.C. also wishes to thank the Spanish Ministry of Education for award of a predoctoral grant (FPU program).

References and notes

1. Koppenol, W. H. *Redox Rep.* **2001**, *6*, 229–234.
2. Welch, K. D.; Davis, T. Z.; Aust, S. D. *Arch. Biochem. Biophys.* **2002**, *397*, 360–369.
3. (a) Fitzpatrick, P. F. *Annu. Rev. Biochem.* **1999**, *68*, 355–381. (b) Massey, V. *J. Biol. Chem.* **1994**, *269*, 22459–22462. (c) Guengerich, F. P. *Chem. Res. Toxicol.* **2001**, *14*, 611–650.
4. Bathelt, C. M.; Ridder, L.; Mulholland, A. J.; Harvey, J. N. *Org. Biomol. Chem.* **2004**, *2*, 2998–3005.
5. Bathelt, C. M.; Schmid, R. D.; Pleiss, J. *J. Mol. Model.* **2002**, *8*, 327–335.
6. White, R. E.; McCarthy, M. B.; Egeberg, K. D. *Arch. Biochem. Biophys.* **1984**, *228*, 493–502.
7. Lewis, D. F. V. *Pharmacogenomics* **2003**, *4*, 387–395.
8. Lewis, D. F. V.; Pratt, J. M. *Drug Metab. Rev.* **1998**, *30*, 739–786.
9. (a) Davydov, D.; Makris, T. M.; Kofman, V.; Werst, D. E.; Sligar, S. G.; Hoffman, B. M. *J. Am. Chem. Soc.* **2001**, *123*, 1403–1415. (b) de Groot, M. J.; Havenith, R. W. A.; Vinkers, H. M.; Zwaams, R.; Vermeulen, N. P. E.; van Lenthe, J. H. *J. Comput. Aided Mol. Des.* **1998**, *12*, 183–193.
10. Schlichting, I.; Berenzen, J.; Chu, K. *Science* **2000**, *287*, 1615–1622.
11. (a) Harman, D. *Proc. Natl. Acad. Sci. U.S.A.* **1981**, *78*, 7124–7128. (b) Ozawa, T. *Physiol. Rev.* **1997**, *77*, 425–464. (c) Beckman, K. B.; Ames, B. N. *Physiol. Rev.* **1998**, *78*, 547–581.
12. Kaur, H.; Halliwell, B. *Anal. Biochem.* **1994**, *220*, 11–15.
13. Collado, D.; Pérez-Inestrosa, E.; Suau, R. *J. Org. Chem.* **2003**, *68*, 3574–3584.
14. The pK_a of tyrosine changes from 10 to −2 upon oxidation (electron release), so the loss of the electron must be accompanied by deprotonation. In nature, the protein controls the reactivity of tyrosine and its radical by modulating the proton transfer reactions that are coupled with electron transfer: (a) Faller, P.; Goussias, C.; Rutherford, A. W.; Un, S. *Proc. Natl. Acad. Sci. U.S.A.* **2003**, *100*, 8732–8735. (b) Stubbe, J. A.; van der Donk, W. A. *Chem. Rev.* **1998**, *98*, 705–762.
15. Bordwell, F. G.; Cheng, J.-P. *J. Am. Chem. Soc.* **1991**, *113*, 1736–1743.
16. (a) Hermann, R.; Naumov, S.; Mahalaxmi, G. R.; Brede, O. *Chem. Phys. Lett.* **2000**, *324*, 265–272. (b) Ganapathi, M. R.; Hermann, R.; Naumov, S.; Brede, O. *Phys. Chem. Chem. Phys.* **2000**, *2*, 4947–4955. (c) Hermann, R.; Naumov, S.; Brede, O. *THEOCHEM* **2000**, *532*, 69–80.
17. (a) Brede, O.; Mehnert, R.; Naumann, W. *Chem. Phys.* **1987**, *115*, 279–290. (b) Guldi, D. M.; Asmus, K. D. *J. Am. Chem. Soc.* **1997**, *119*, 5744–5745.
18. (a) Yi, M.; Scheiner, S. *Chem. Phys. Lett.* **1996**, *262*, 567–572. (b) Dixon, W. T.; Murphy, D. *J. Chem. Soc., Faraday Trans. 2* **1976**, *72*, 1221–1230. (c) Bordwell, F. G.; Cheng, J. P. *J. Am. Chem. Soc.* **1991**, *113*, 1736–1743.
19. Luo, Y.-R. *Handbook of Bond Dissociation Energies in Organic Compounds*; CRC: Boca Raton, FL, 2003.
20. Nagaoka, S.; Kuranaka, A.; Tsuboi, H.; Hagashima, U.; Mukai, K. *J. Phys. Chem.* **1992**, *96*, 2754–2761.
21. (a) *Essentials of Molecular Photochemistry*; Gilbert, A., Baggott, J., Eds.; Blackwell: Oxford, UK, 1991. (b) Said, A. H.; Mhalla, F. M.; Amatore, C.; Verpeaux, J.-N. *J. Electroanal. Chem.* **1999**, *464*, 85–92.
22. (a) Frisch, M. J.; Trucks, G. W.; Schlegel, H. B.; Scuseria, G. E.; Robb, M. A.; Cheeseman, J. R.; Zakrzewski, V. G.; Montgomery, J. A.; Stratman, R. E.; Burant, S.; Dapprich, J. M., Millam, J. M.; Daniels, A. D.; Kudin, K. N.; Strain, M. C.; Farkas, O.; Tomasi, J.; Barone, V.; Cossi, M.; Cammi, R.; Mennucci, B.; Pomelli, C.; Adamo, C.; Clifford, S.; Ochterski, G.; Petersson, A.; Ayala, P. Y.; Cui, Q.; Morokuma, K.; Malick, D. K.; Rabuck, A. D.; Raghavachari, K.; Foresman, J. B.; Cioslowski, J.; Ortiz, J. V.; Stefanov, B. B.; Liu, G.; Liashenko, A.; Piskorz, I.; Komaromi, I.; Gomperts, R.; Martin, R. L.; Fox, D. J.; Keith, T.; Al-Laham, M. A.; Peng, C. Y.; Manayakkara, A.; Gonzalez, C.; Challacombe, M.; Gill, P. M. W.; Johnson, B. G.; Chen, W.; Wong, M. W.; Andres, J. L.; Head-Gordon, M.; Replogle, E. S.; Pople, J. A. *Gaussian 98*, Revision A.1; Gaussian, Inc.: Pittsburgh, PA, 1998. (b) Becke, A. D. *J. Chem. Phys.* **1993**, *98*, 5648–5652. (c) Quin, Y.; Wheeler, R. A. *J. Phys. Chem.* **1996**, *100*, 10554–10563. (d) Pietro, W. J.; Francl, M. M.; Hehre, W. J.; Defrees, D. J.; Pople, J. A.; Binkley, J. S. *J. Am. Chem. Soc.* **1982**, *104*, 5039–5048.
23. (a) Joshi, R.; Naumov, S.; Kapoor, S.; Mukherjee, T.; Hermann, R.; Brede, O. *J. Phys. Org. Chem.* **2004**, *17*, 665–674. (b) Brede, O.; Kapoor, S.; Mukherjee, T.; Hermann, R.; Naumov, S. *Phys. Chem. Chem. Phys.* **2002**, *4*, 5096–5104.
24. Dey, G. R.; Hermann, R.; Naumov, S.; Brede, O. *Chem. Phys. Lett.* **1999**, *310*, 137–144.
25. Dale, W. J.; Hennis, H. E. *J. Am. Chem. Soc.* **1956**, *78*, 2543–2547.
26. Levacher, V.; Moberg, C. *React. Polym.* **1995**, *24*, 183–193.
27. Gibson, H. W.; Popp, F. D. *J. Chem. Soc. (C)* **1966**, 1860–1864.
28. Carr, J. A.; Bisht, K. S. *Org. Lett.* **2004**, *6*, 3297–3300.
29. Collado, D.; Pérez-Inestrosa, E.; Suau, R.; Desvergne, J.-P.; Bouas-Laurent, H. *Org. Lett.* **2002**, *4*, 855–858.
30. Kawai, H.; Kotake, Y.; Ohta, S. *Chem. Res. Toxicol.* **2000**, *13*, 1294–1301.